Fracture toughness of Si_3N_4 measured with short bar chevron-notched specimens

JONATHAN A. SALEM, JOHN L. SHANNON Jr,
Fracture Research Section, National Aeronautics and Space Administration, Lewis Research Center, Cleveland, Ohio 44135, USA

The short bar chevron-notched specimen was used to measure the plane strain fracture toughness of hot-pressed Si_3N_4. Specimen proportions and chevron-notch angle were varied, thereby varying the amount of crack extension to maximum load (upon which K_{IC} was based). The measured toughness ($4.68 \pm 0.19\,MN\,m^{3/2}$) was independent of these variations, inferring that the material has a flat crack growth resistance curve.

Nomenclature

a	crack length
a_A	crack length at arrest of unstable crack advance
a_1	length of chevron notch at specimen surface (distance from line of load application to point of chevron emergence at specimen surface)
a_0	initial crack length (distance from line of load application to tip of chevron)
a_R	crack length at ending of stable crack extension (conversely, crack length at onset of abrupt, unstable crack advance)
B	specimen thickness
H	specimen half-height
K_{IA}	stress intensity factor at arrest of unstable crack advance
K_{IR}	stress intensity factor at end of stable crack extension (crack growth resistance)
K_{IC}	plane strain fracture toughness
P_{max}	maximum applied load in fracture toughness test
W	specimen width
Y^*	dimensionless stress intensity factor coefficient for chevron-notched specimen
Y^*_m	minimum value of Y^* as a function of α
α	a/W
α_0	a_0/W
α_1	a_1/W

1. Introduction

There is currently no standardized method of test for determining the plane strain fracture toughness of brittle nonmetallic materials. Specimens and procedures vary from laboratory to laboratory, often resulting in differing indications of fracture toughness for a given material [1, 2].

The principal difficulties with fracture toughness testing brittle nonmetallics are introducing a controlled precrack in a reproducible manner, and measuring the length of the precrack when it can be successfully introduced. These difficulties are circumvented by the use of chevron-notched specimens proposed by Barker [3] and based on earlier work of Nakayama [4] and Tattersall and Tappin [5]. On testing the specimen, a crack develops at the chevron tip and extends stably as the load is increased. For a given specimen and chevron-notched geometry, maximum load always occurs at the same relative crack length providing the material has a flat crack growth resistance curve. Fracture toughness, K_{IC}, is determined from the maximum load with no need for crack-length measurement.

We have previously developed the P_{max}–K_{IC} relationships for the short bar, short rod, and four-point bend specimens shown in Fig. 1 [6–10]. A summary of recent analyses appears in [1]. We examined the performance of chevron-notched specimens [12–14] when their size, proportions, and chevron-notch geometries were varied. Extensive results on Al_2O_3 showed material to have a rising crack growth resistance curve. More limited results on Si_3N_4 suggested that it has a flat crack growth resistance curve. The

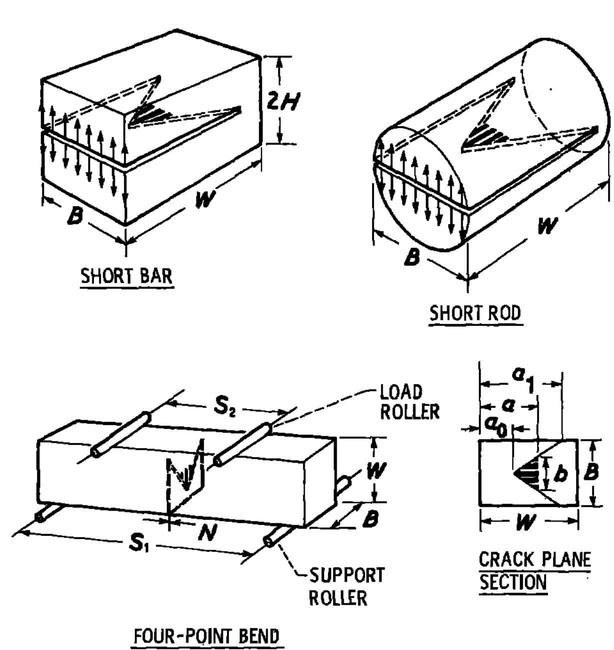

Figure 1 Family of chevron-notched fracture toughness test specimens.

 © *1987 Chapman and Hall Ltd.*

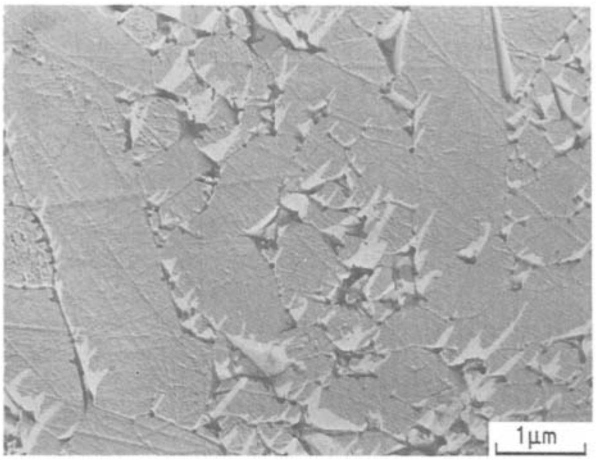

Figure 2 Transmission electron micrograph of investigated NC-132 hot-pressed silicon nitride.

purpose of the present study was to broaden the investigation of the fracture toughness of Si_3N_4 using the short bar chevron-notched specimen to substantiate the prior indication that it has a flat crack growth resistance curve.

2. Material and procedure

The material investigated was Norton Company NC-132 hot-pressed silicon nitride (Si_3N_4), received as a single 150 mm × 150 mm × 10 mm plate with a measured density of 3.25 g cm^{-3}. Its microstructure (Fig. 2) is a mixture of equiaxed and elongated grains. The equiaxed grains ranged in size from 0.1 to 1.0 μm, and the elongated grains from 0.15 to 2.0 μm in width at an aspect ratio of 1 : 2 to 1 : 6.

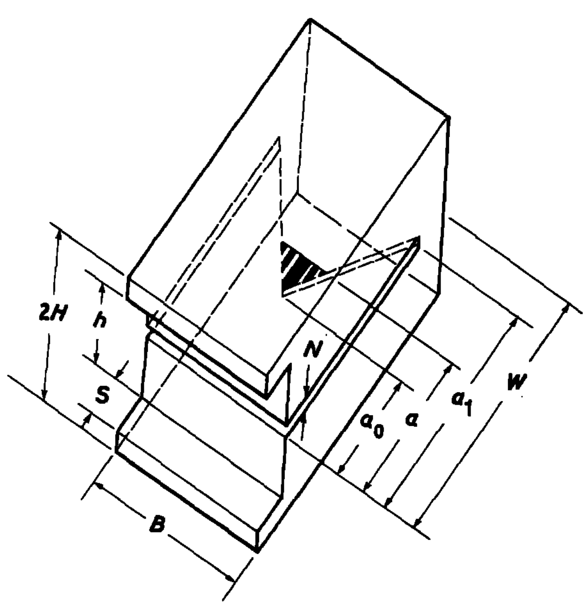

$B = 2H$	W	$W/2H$	h	S	N	a_0	a_1
8.9	13.3	1.5	4.6	1.9	0.3	2.5 – 6.8	13.3
8.9	15.1	1.7	4.6	1.9	0.3	3.1 – 7.7	15.1
8.9	17.8	2.0	4.6	1.9	0.3	3.4 – 8.9	17.8

Figure 3 Dimensions of short bar chevron notched fracture toughness test specimens used in this investigation. (All dimensions in mm.)

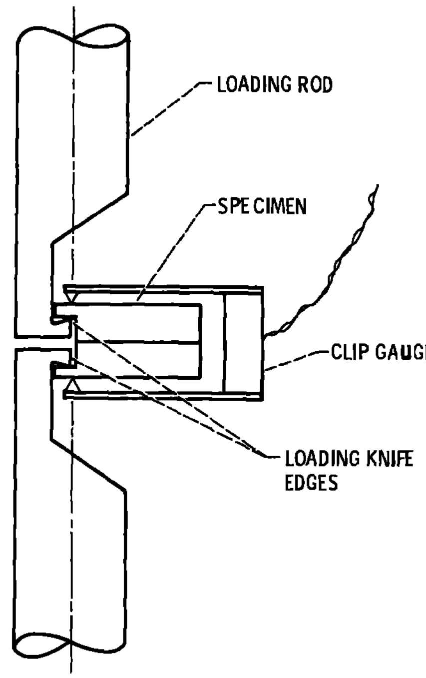

Figure 4 Test apparatus.

Short bar specimens were machined from the plate to the dimensions shown in Fig. 3, all with their long axes parallel to the same plate edge and their notch plane parallel to the plate surface. Specimen proportions (width-to-height, $W/2H$ ratios) ranged from 1.5 to 2.0. The chevron-notch length at the specimen surface (a_1) was always made equal to the specimen width (W), (that is, $\alpha_1 = 1$). The chevron angle was varied by varying the length of the chevron tip (a_0). The initial relative crack (notch) length ranged from 0.2 to 0.5. The notches were introduced by diamond wheel slotting with a kerf (slot width, N) ranging from 0.31 to 0.43 mm.

The test apparatus is shown in Fig. 4. Care was exercised in aligning the loading rods according to a procedure previously used by the authors for compliance calibrations of the short bar specimen [6]. Crack opening displacement was measured with an ASTM E-399 clip-in displacement gauge modified by the placement of hardened steel cones on the inner surfaces of the gauge arms. The cones were set into a pair of small indentations in the specimen's plane of loading on the top and bottom surfaces of the specimen. The clip gauge force was tared from the load measurement, and the specimen was installed by pressing it firmly against the loading rods to seat the loading knife edges in the corners of the specimen loading grooves.

Temperature of the laboratory air during the period of test ranged from 74 to 78° F (~23 to 26° C) and the relative humidity ranged from 40 to 60%. Specimen load was applied at a controlled constant stroke rate of 0.05 mm min^{-1}. Two types of load against displacement records were obtained. One type is shown in Fig. 5. The trace is initially linear. The slope decreases as stable crack extension occurs, interrupted periodically by sudden drops due to bursts of unstable crack extension. These increments of alternating stable and unstable crack extension are discernible on the

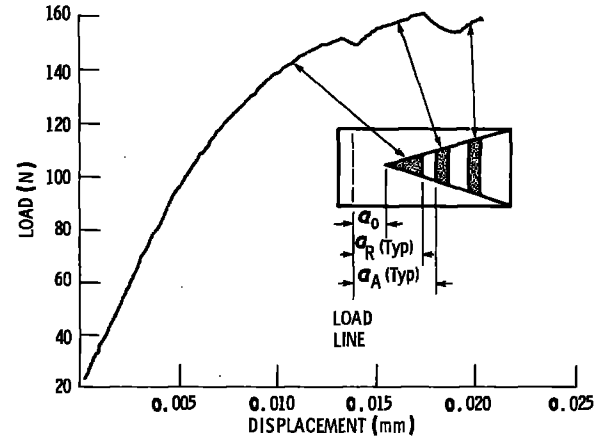

Figure 5 Load displacement diagram exhibiting stable and unstable crack extension.

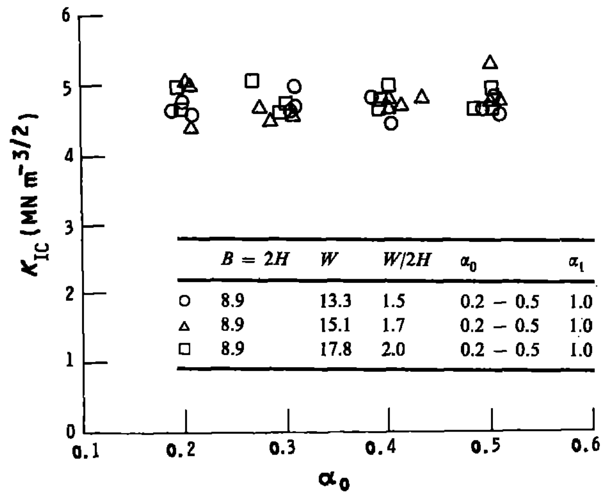

	$B = 2H$	W	$W/2H$	α_0	α_1
○	8.9	13.3	1.5	0.2 – 0.5	1.0
△	8.9	15.1	1.7	0.2 – 0.5	1.0
□	8.9	17.8	2.0	0.2 – 0.5	1.0

Figure 6 Effects of α_0 and W/H on the K_{IC} of hot-pressed silicon nitride (NC-132) determined with short bar chevron notched specimens.

fracture surface as alternating bands of contrasting texture, as shown schematically in the inset. The second type of test record differed in that no load drops (unstable crack bursts) occurred.

The plane strain fracture toughness, K_{IC}, was calculated from the maximum test load and minimum value of the stress intensity factor coefficient, Y_m^*, under the assumption of a flat crack growth resistance curve, using the following wide-range expression for Y_m^* from Bubsey *et al.* [10]:

$$\begin{aligned} Y_m^* = & -17.03 + 14.97(W/H) - 1.25(W/H)^2 \\ & + [-116 + 70.80(W/H) - 7.4(W/H)^2]\alpha_0 \\ & + [1131 - 652(W/H) + 85.5(W/H)^2]\alpha_0^2 \\ & + [-1351 + 827(W/H) - 110.8(W/H)^2]\alpha_0^3 \end{aligned} \quad (1)$$

This expression is applicable for the following range of specimen dimensional parameters: $1.5 \leqslant W/2H \leqslant 2.0$, $0 \leqslant \alpha_0 \leqslant 0.5$, and $\alpha_1 = 1$.

The crack length, a, was measured at each marking on the fracture surface of those specimens that exhibited periodic unstable crack jumps. Conjugate values of load and crack length were used to compute K_I at the onset and arrest of each unstable crack burst. The data were examined for possible characteristic values of K_I corresponding to each event. The following expressions for Y^* were used for these calculations:

$$\begin{aligned} Y^* = \exp [& (3.329 + 1.026\alpha_0 + 78.21\alpha_0^2) \\ & + (-0.812 - 58.08\alpha_0 - 334.4\alpha_0^2)\alpha \\ & + (-2.061 + 265.26\alpha_0 + 461.4\alpha_0^2)\alpha^2 \\ & + (4.35 - 417.12\alpha_0 - 156.1\alpha_0^2)\alpha^3 \\ & + (0.349 + 219.8\alpha_0 - 65.55\alpha_0^2)\alpha^4] \end{aligned} \quad (2)$$

for $W/2H = 1.5$, $0.1 \leqslant \alpha_0 \leqslant 0.35$, $\alpha_1 = 1$, and $\alpha_0 \leqslant \alpha \leqslant 0.8$, and

$$\begin{aligned} Y^* = \exp [& (4.308 + 4.757\alpha_0 + 83.77\alpha_0^2) \\ & + (-6.529 - 19.19\alpha_0 - 358.7\alpha_0^2)\alpha \\ & + (-16.63 + 172.0\alpha_0 + 483.1\alpha_0^2)\alpha^2 \\ & + (-22.17 - 313.0\alpha_0 - 151.1\alpha_0^2)\alpha^3 \\ & + (13.22 + 173.7\alpha_0 - 72.71\alpha_0^2)\alpha^4] \end{aligned} \quad (3)$$

for $W/2H = 2.0$, $0.1 \leqslant \alpha_0 \leqslant 0.35$, $\alpha_1 = 1$, and $\alpha_0 \leqslant \alpha \leqslant 0.8$.

The above equations were developed from experimental compliance measurements [10]. Their ranges of validity are limited. Some of the crack growth resistance analyses in this study were outside those ranges, and in those instances the following generalized expression was used, [13];

$$\begin{aligned} Y^* = & \frac{\alpha}{(1-\alpha)^{3/2}} \left[\ln \left(\exp \left[\frac{2.702}{\alpha} + 1.628 \right] \right. \right. \\ & + \exp \left\{ \left[12 \frac{W^3(1-\alpha)^3}{H^3} \right]^{1/2} \right. \\ & \left. \left. \left. \times \left[1 + \frac{0.679}{\alpha(W/H)} \right] \right\} \right) \right] \left[\frac{\alpha_1 - \alpha_0}{\alpha - \alpha_0} \right]^{1/2} \end{aligned} \quad (4)$$

This expression was developed by exponential superposition of solutions for relatively short and relatively long straight-through cracks and assuming that the change is compliance with change in relative crack length for a chevron-notched specimen is equal to that for a straight-through notched (cracked) specimen.

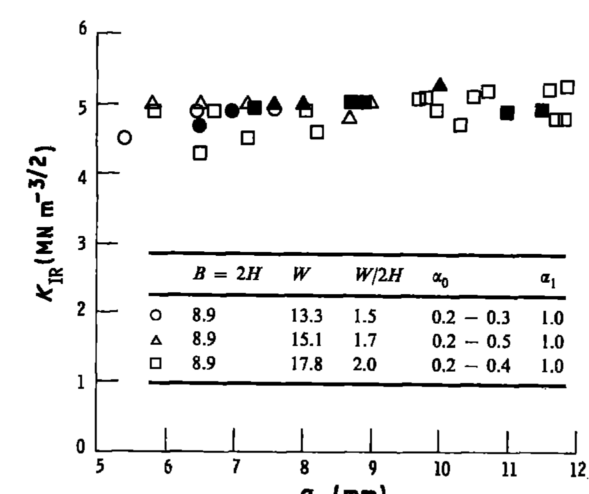

	$B = 2H$	W	$W/2H$	α_0	α_1
○	8.9	13.3	1.5	0.2 – 0.3	1.0
△	8.9	15.1	1.7	0.2 – 0.5	1.0
□	8.9	17.8	2.0	0.2 – 0.4	1.0

Figure 7 Crack growth resistance as a function of crack length.

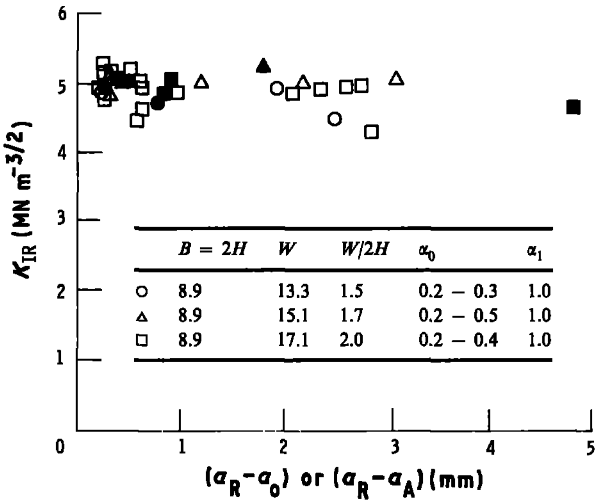

Figure 8 Crack growth resistance as a function of the stable crack growth increment.

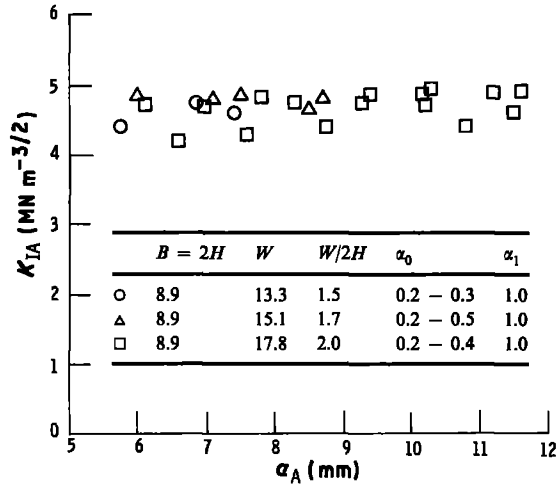

Figure 9 Crack arrest stress intensity as a function of the arrested crack length.

3. Results and discussion

The primary result of this investigation is presented in Fig. 6. As suggested by our earlier results [12], there is no effect on K_{IC} of varying the specimen proportions or chevron-notch angle. Such variations alter the amount of crack extension to maximum load (the measurement point). It may be inferred from the absence of an effect that the crack growth resistance curve for this material is flat; i.e. $K_{IC} \neq f(\Delta a)$. The value of K_{IC} derived from the total population of data in Fig. 6 is $4.68 \pm 0.19\,\mathrm{MN\,m^{-3/2}}$.

The test records exhibiting sudden load drops corresponding to periodic bursts of unstable crack extension were given an additional analysis. K_I was calculated for the peaks of each serration in the load against displacement trace. These we designate K_{IR}, and are plotted in Fig. 7 as a function of the corresponding crack length (a_R) and in Fig. 8 as a function of the crack extension increment ($a_R - a_0$) for the first increment and ($a_R - a_A$) for succeeding increments. Closed symbols denote combinations of P_{max} and the corresponding crack length, and are in fact K_{IC}. The value of K_{IC} for this population of specimens is $4.96 \pm 0.19\,\mathrm{MN\,m^{-3/2}}$. The open symbols denote all other combinations of load peaks and corresponding crack lengths and may be considered the conventional "crack growth resistance". Their value is $4.92 \pm 0.22\,\mathrm{MN\,m^{-3/2}}$, essentially equal to K_{IC} and therefore consistent with the inferrence of a flat crack growth resistance curve for this material.

K_I at the arrest of each unstable crack burst (we designate K_{IA}) is plotted in Fig. 9 as a function of the arrest-crack length. The value of K_{IA} is $4.70 \pm 0.23\,\mathrm{MN\,m^{-3/2}}$, 4.5% less than K_{IR}. This difference will depend, of course, on the crack velocity and the response of the loading system. There probably is no significance to this quantity K_{IA}. Prior study [15] has shown that reaction-bonded silicon nitride under dynamic loading conditions exhibits no tendency to crack-arrest.

4. Conclusion

The plane strain fracture toughness, K_{IC}, of NC-132 Si_3N_4 measured at room temperature using short bar chevron-notched specimens is independent of the amount of crack extension to maximum load (the measurement point), such crack extension having been varied by varying specimen proportions and chevron-notch angle. It is concluded that NC-132 Si_3N_4 has a flat crack growth resistance curve at room temperature.

References

1. D. MUNZ, in "Fracture Mechanics of Ceramics", Vol. 6, edited by R. C. Bradt, A. G. Evans, D. P. H. Hasselman and F. F. Lange (Plenum, New York, 1983) pp. 1–26.
2. S. W. FREIMAN, *ibid.*, pp. 27–45.
3. L. M. BARKER, *Eng. Fract. Mech.* **9** (1977) 361.
4. J. NAKAYAMA, *J. Amer. Ceram. Soc.* **48** (1965) 583.
5. H. G. TATTERSALL and G. TAPPIN, *J. Mater. Sci.* **1** (1966) 296.
6. D. MUNZ, R. T. BUBSEY and J. E. SRAWLEY, *Int. J. Fract.* **16** (1980) 359.
7. R. T. BUBSEY, D. MUNZ, W. S. PIERCE and J. L. SHANNON Jr, *ibid.* **18** (1982) 125.
8. J. L. SHANNON Jr, R. T. BUBSEY and W. S. PIERCE, *ibid.* **19** (1982) R55.
9. D. G. MUNZ, J. L. SHANNON Jr and R. T. BUBSEY, *ibid.* **16** (1980) R137.
10. R. T. BUBSEY, W. S. PIERCE and J. L. SHANNON Jr, "Closed-Form Expressions for Crack-Mouth Displacements and Stress Intensity Factors for Chevron-Notched Short Bar and Short Rod Specimens Based on Experimental Compliance Measurements", NASA TM-83796 (1985).
11. J. H. UNDERWOOD, S. W. FREIMAN, and R. I. BARATTA (eds), "Chevron-Notched Specimens: Testing and Stress Analysis", ASTM STP-855 (American Society for Testing and Materials, Philadelphia, 1984).
12. D. MUNZ, R. T. BUBSEY and J. L. SHANNON Jr, *J. Test. Eval.* **8** (1980) 103.
13. J. L. SHANNON Jr, R. T. BUBSEY, D. MUNZ and W. S. PIERCE, in "Advances in Fracture Research", Vol. 2, edited by D. Francois (Pergamon, New York, 1982) pp. 1127–41.
14. J. L. SHANNON Jr and D. MUNZ, in "Chevron-Notched Specimens: Testing and Stress Analysis", ASTM STP-855, edited by J. H. Underwood, S. W. Freiman, and F. I. Baratta (American Society for Testing and Materials, Philadelphia, 1984) pp. 270–80.
15. A. S. KOBAYASHI, A. F. EMERY and B. W. LIAW, *J. Amer. Ceram. Soc.* **66** (1983) 151.

Received 2 December 1985
and accepted 22 May 1986